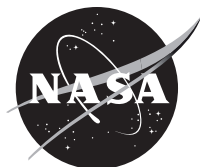NASA/TM—2019-220165

Reducing Aviation Fuel Costs With Non-Destructive Testing

Peter J. Schemmel
Glenn Research Center, Cleveland, Ohio

April 2019

NASA STI Program . . . in Profile

Since its founding, NASA has been dedicated to the advancement of aeronautics and space science. The NASA Scientific and Technical Information (STI) Program plays a key part in helping NASA maintain this important role.

The NASA STI Program operates under the auspices of the Agency Chief Information Officer. It collects, organizes, provides for archiving, and disseminates NASA's STI. The NASA STI Program provides access to the NASA Technical Report Server—Registered (NTRS Reg) and NASA Technical Report Server—Public (NTRS) thus providing one of the largest collections of aeronautical and space science STI in the world. Results are published in both non-NASA channels and by NASA in the NASA STI Report Series, which includes the following report types:

- TECHNICAL PUBLICATION. Reports of completed research or a major significant phase of research that present the results of NASA programs and include extensive data or theoretical analysis. Includes compilations of significant scientific and technical data and information deemed to be of continuing reference value. NASA counter-part of peer-reviewed formal professional papers, but has less stringent limitations on manuscript length and extent of graphic presentations.

- TECHNICAL MEMORANDUM. Scientific and technical findings that are preliminary or of specialized interest, e.g., "quick-release" reports, working papers, and bibliographies that contain minimal annotation. Does not contain extensive analysis.

- CONTRACTOR REPORT. Scientific and technical findings by NASA-sponsored contractors and grantees.

- CONFERENCE PUBLICATION. Collected papers from scientific and technical conferences, symposia, seminars, or other meetings sponsored or co-sponsored by NASA.

- SPECIAL PUBLICATION. Scientific, technical, or historical information from NASA programs, projects, and missions, often concerned with subjects having substantial public interest.

- TECHNICAL TRANSLATION. English-language translations of foreign scientific and technical material pertinent to NASA's mission.

For more information about the NASA STI program, see the following:

- Access the NASA STI program home page at http://www.sti.nasa.gov

- E-mail your question to help@sti.nasa.gov

- Fax your question to the NASA STI Information Desk at 757-864-6500

- Telephone the NASA STI Information Desk at 757-864-9658

- Write to:
  NASA STI Program
  Mail Stop 148
  NASA Langley Research Center
  Hampton, VA 23681-2199

Reducing Aviation Fuel Costs
With Non-Destructive Testing

Peter J. Schemmel
Glenn Research Center, Cleveland, Ohio

Acknowledgments

This report contains preliminary findings,
subject to revision as analysis proceeds.

Trade names and trademarks are used in this report for identification
only. Their usage does not constitute an official endorsement,
either expressed or implied, by the National Aeronautics and
Space Administration.

Level of Review: This material has been technically reviewed by technical management.

Available from

NASA STI Program
Mail Stop 148
NASA Langley Research Center
Hampton, VA 23681-2199

National Technical Information Service
5285 Port Royal Road
Springfield, VA 22161
703-605-6000

This report is available in electronic form at http://www.sti.nasa.gov/ and http://ntrs.nasa.gov/

Reducing Aviation Fuel Costs With Non-Destructive Testing

Peter J. Schemmel
National Aeronautics and Space Administration
Glenn Research Center
Cleveland, Ohio 44135

Abstract

Thermal barrier coatings (TBCs) are absolutely critical to the efficient and safe operation of gas turbine engines (GTEs). Manufacturing TBCs is a complex chemical, thermal and mechanical process that requires precise control. And yet, the variation in life of a TBC operated within a GTE is large. This variation ultimately reduces operational performance via a designed reduction to the turbine entry temperature, T_4.

This paper makes the case for developing advanced THz and submillimeter based non-destructive testing (NDT) techniques, capable of estimating when TBC components will fail. Such a technique could identify TBCs with low expected remaining useful lifetimes, directly after production. These TBCs could be remanufactured, thereby not only improving their own expected useful life, but also the mean lifetime of the entire manufacturing population. A series of calculations demonstrates that TBCs with enhanced life characteristics can withstand higher T_4 temperatures. Assuming that a GTE is to operate at a constant thrust, this increased temperature can be traded for a reduction in fuel flow. An analysis comparing fuel savings to manufacturing costs shows that substantial savings are achievable.

1.0   Introduction

Gas turbine engines (GTEs) were first developed in the late 1930s, and at the time were producing around 1,000 lb of thrust (Ref. 1). Today, GTEs are capable of producing over 70,000 lb of thrust. In the 1960s turbofan bypass ratios were typically less than two, while today, bypass ratios above 10 are the norm (Ref. 2). Next generation designs aim to improve overall efficiency by pushing the boundaries of material properties. For example, combustion temperatures today already exceed the melting point of the combustor and first stage turbine blades, and yet they are continuing to rise.

There are several reasons for designing GTEs to run at increased combustion temperatures. For example, hotter combustion is a byproduct of running a lean fuel to air mixture, which reduces fuel consumption. In addition, higher combustion temperatures increase the amount of energy available for the turbine to extract, thereby increasing thrust (Ref. 3). This increased thrust can be used to power a larger fan, resulting in an increased bypass ratio. Achieving these benefits however, requires further advancements in material durability.

Thermal barrier coatings (TBCs) play a crucial role in enabling future GTE designs. Modern GTEs use TBCs to protect combustors and first stage turbine blades from the harsh environment in which they operate. TBCs are incredible materials. In the case of turbine blades, the TBC must support large thermal gradients between hot gas on their outer surface and relatively "cool," air being pumped through inner substrate cooling channels. In addition, TBCs must closely match the thermal expansion properties of the substrate superalloy. Ultimately, TBCs form a highly complex mechanical, chemical and thermal structure, with the material they are protecting. Because TBCs are so complex, understanding how they fail is a challenge (Refs. 4 to 6).

Since TBCs are critical to safe GTE operations, their maintenance schedules are calculated based on the worst performing TBC lifetimes. Once the scheduled service time is reached, TBC coated turbine blades are replaced. This is of course inefficient because by definition, a large majority of blades do not need to be replaced. However, safety is the primary concern with GTE design, and so good TBCs are sacrificed.

This paper explores the impact of reducing the number of TBC coated turbine blades with poor expected life performance that enter service. Despite increasing mean service life of the component population, it is assumed that GTE maintenance schedules will remain unchanged. As such, this paper takes the following approach. First, an increased mean lifetime (durability) implies that TBCs will survive at higher turbine entry temperatures (T_4). Increased T_4 is then traded for a larger bypass ratio, and therefore a reduced fuel flow. The cost to increase TBC durability is compared to the savings from reduced fuel usage, to obtain an optimal number of TBC components to remanufacture. The paper concludes by identifying how non-destructive-testing (NDT) techniques currently under development, could be used to make this concept a reality.

2.0   Cost Incurred to Remanufacture TBCs

Consider a manufactured population of TBC coated turbine blades. The failure probability of this population follows a three-parameter Weibull distribution,

$$f(t) = \frac{\beta}{\eta}\left(\frac{t-\gamma}{\eta}\right)^{\beta-1} \cdot \exp\left[-\left(\frac{t-\gamma}{\eta}\right)^{\beta}\right]. \qquad (1)$$

Here, $f(t)$ is the failure probability at time t, β is the shape parameter, η is the characteristic life and γ is the failure free life. The mean of the distribution is,

$$\bar{t} = \eta \cdot \Gamma\left(\frac{1}{\beta}+1\right), \qquad (2)$$

and the standard variation is,

$$\sigma = \eta \cdot \sqrt{\Gamma\left(\frac{2}{\beta}+1\right) - \Gamma\left(\frac{1}{\beta}+1\right)^2}, \qquad (3)$$

where Γ is the gamma function. Reasonable numbers for TBC coated turbine blades are $\beta = 4$, $\eta = 1{,}400$ (hours) and $\gamma = 0$ (Ref. 7).

Imagine an NDT technique capable of measuring the expected remaining useful life of TBC components directly after manufacturing. If this were possible, TBCs with the least amount of useful life (i.e., those that fail early) could be removed from the production line. Removed components are recoated (or remanufactured) and reintroduced, to maintain a constant production lot size. This process increases the population's mean lifetime, while reducing lifetime variations.

Increased mean lifetime is quantified by first creating a sample component population from a three-parameter Weibull distribution. The size of the population is N_P. The manufacturing process produces some components (N_R), which do not meet the specification for expected useful life. These components are removed, recoated and reintroduced into the population. The number of components with acceptable lifetimes is the manufacturing yield, $N_Y = N_P - N_R$.

(a) Probability density function

(b) Survival function

(c) Mean lifetime difference as a function of E_R

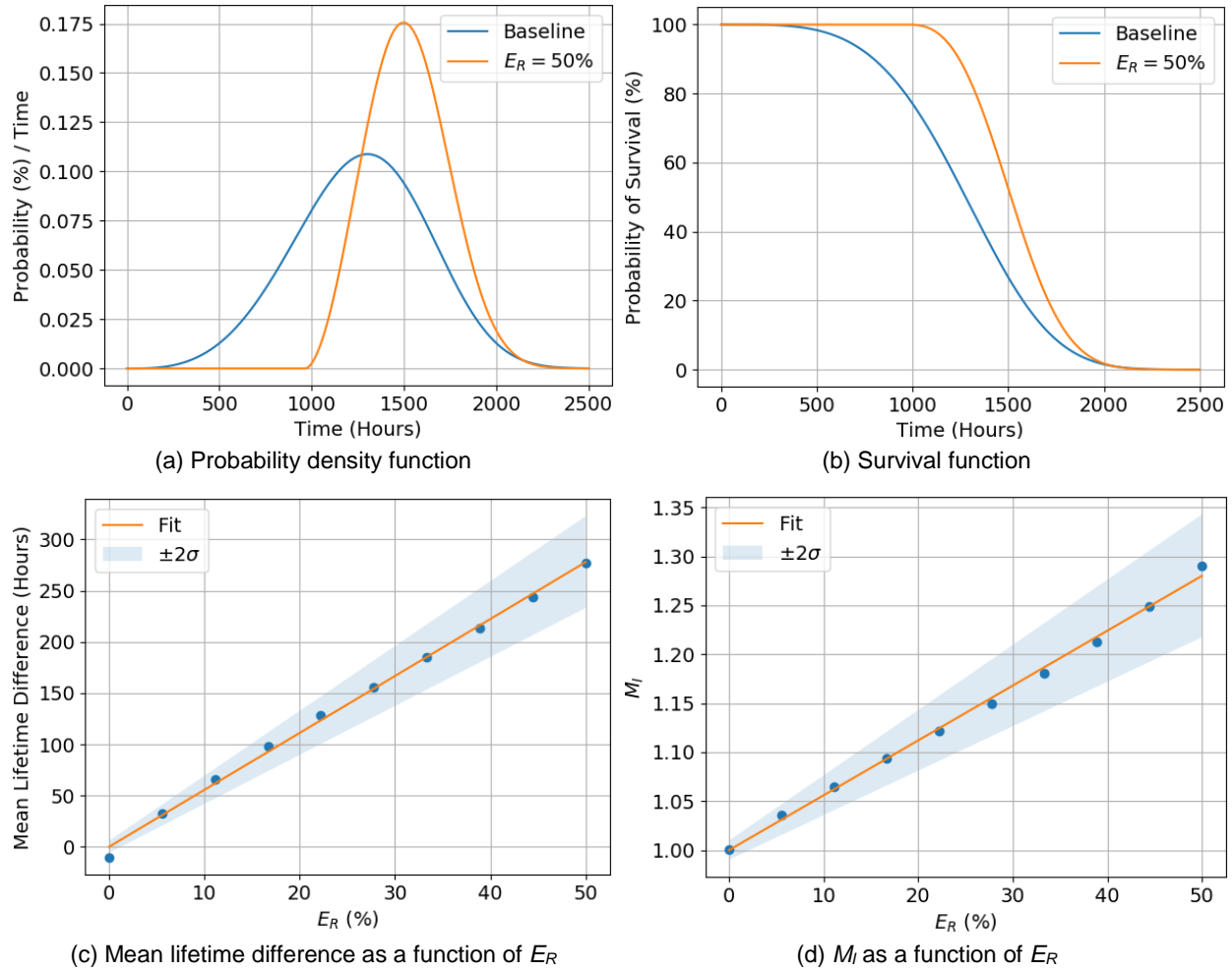(d) M_I as a function of E_R

Figure 1.—Identifying and removing TBCs with low expected remaining life increases the overall mean lifetime and reduces lifetime variations, of the population (a), resulting in an improved TBC survivability rate (b). The improvement in mean life is a linear function of the exchange rate (c), which is also true of the adjusted lifetime ratio parameter M_I (d).

The modified population's new mean lifetime Equation (2) is calculated by refitting the population with a new three-parameter Weibull distribution. Figure 1(a) shows an original, and modified, Weibull distribution clearly demonstrating the improvement in mean lifetime and reduction in lifetime variation. This assertion is further supported by examining the survival functions Figure 1(b). Data shown in Figure 1 was generated by averaging the results of 100 tests, using a distribution size of 5,000 elements, in order to ensure quality of the fitting procedure.

The improvement in mean lifetime is plotted against the exchange rate ($E_R = N_R/N_P$) in Figure 1(c), and the relationship is clearly linear. Note that the blue shaded region denotes $\pm 2\sigma$ on either side of the fit result, and is carried through the remaining calculations. For reasons that will become apparent in the

upcoming section, knowledge of the parameter $M_I = \overline{t_1}\big/\left(2\overline{t_1} - \overline{t_2}\right)$, as a function of the exchange rate is

of interest. The parameters $\overline{t_1}$ and $\overline{t_2}$ are the respective mean lifetimes of the original and modified distributions. It will be shown in the upcoming section that M_I is a ratio of lifetimes that accounts for increased TBC durability. Figure 1(d) shows that this relationship is approximated well by a linear function.

Exchanging components clearly benefits the statistical life performance of the population. However, this process requires additional manufacturing steps, and therefore, the increase in performance comes at a cost. This cost is calculated by determining the total number of components remanufactured as a function of the exchange rate. The initial number of components needing to be remanufactured is N_R, and the probability of success is assumed to be equal to that of the original manufacturing process, namely, $P = N_Y/N_P$. The process is repeated until there are no longer any components that require remanufacturing.

The number of components unsuccessfully recoated during cycle "i" is,

$$N'_{R_i} = N_R (1 - P) = N_R - (E_R \cdot N_Y).$$

(4)

The process is repeated until $N'_{R_i} = 0$, such that the total number of recoated components is,

$$N_T = N_R + \sum_{i=0}^{n} N'_{R_i}.$$

(5)

Figure 2 shows how manufacturing costs increase as a function of the exchange rate, assuming a population size of $N_P = 100$ and a fixed recoating cost per turbine blade of \$750. A cubic function was used to fit simulated data from 1,000 individual runs, and the shaded region depicts a region of variation between ±2σ of the average fit.

3.0   Increasing Turbine Entry Temperature

The previous section demonstrated how TBC mean lifetimes are increased, and variations in those lifetimes reduced, by measuring the expected remaining useful life of a TBC using a hypothetical NDT technique. Those TBCs with expected lifetimes below a specification threshold are exchanged for TBCs that meets the requirements. This section will examine how increasing TBC mean lifetime translates to an increase in T_4.
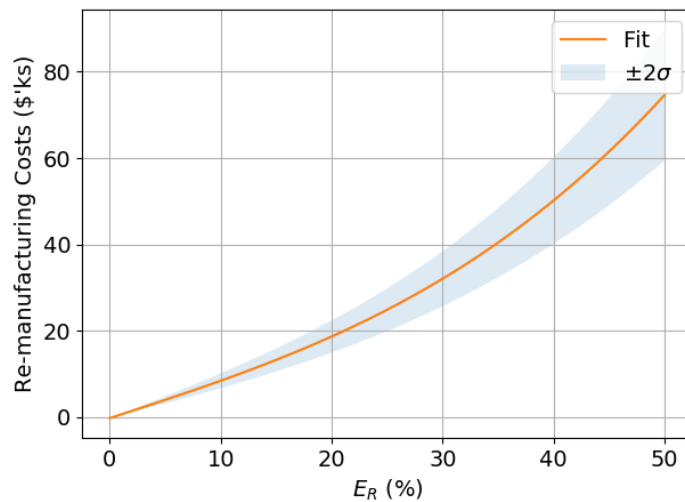

Figure 2.—The number of components manufactured increases non-linearly with the exchange rate, and therefore increases the manufacturing costs.

TABLE I.—TBC-TGO PARAMETERS

Parameter	Units
A_0..	10^{-6} m/s^q
q	0.332
Q_0	766,900 J/mol
Θ_R...	2424 K

To accomplish this, TBC failure must be understood, yet it is a complex process and there are several documented failure modes (Refs. 4 and 8). Excluding cases of impact damage or interaction with foreign materials, TBCs primarily fail due to growth of a thermally grown oxide (TGO) layer. TGOs live between the TBC's bondcoat and topcoat. The TGO layer grows as the TBC undergoes thermal cycling, and this growth produces out of plane stresses due to substrate surface undulations. These stresses build up over time and start to form small cracks. As thermal cycles continue to build up over time, the small cracks begin to form networks, and eventually a large portion of TBC will spall, resulting in failure.

TGO growth can be described as a function of 1) the peak thermal cycle temperature (which will be set to T_4 in this analysis) and 2) the accumulated time exposed to that temperature, t. The TGO height h is then (Refs. 9 to 12),

$$h = A_0 t^q \cdot \exp\left[\frac{Q_0}{R} \cdot \left(\frac{1}{\Theta_R} - \frac{1}{T_4}\right)\right],$$
(6)

where A_0 is a proportionality constant, q is a growth exponent, Q_0 is the apparent activation energy, R is the universal gas constant and Θ_R is a reference temperature. Typical values for these parameters are shown in Table I, (Ref. 7).

Consider two identical TBCs, A and B, operated in different environments. Let each TBC experience a different T_4 and accumulated cycle time t. The TGO height for each is,

$$h_A = A_0 \overline{t_A}^q \cdot \exp\left[\frac{Q_0}{R} \cdot \left(\frac{1}{\Theta_R} - \frac{1}{T_{4A}}\right)\right]$$

$$h_B = A_0 \overline{t_B}^q \cdot \exp\left[\frac{Q_0}{R} \cdot \left(\frac{1}{\Theta_R} - \frac{1}{T_{4B}}\right)\right]$$
(7)

Remember, TBC failure is driven by TGO growth. Therefore, the TGO thicknesses at failure are equivalent,

$$h_A = h_B.$$
(8)

After expanding and rearranging terms, Equation (8) becomes,

$$\left(\frac{\overline{t_A}}{\overline{t_B}}\right)^q = \exp\left[\frac{Q_0}{R}\left(\frac{1}{T_{4A}} - \frac{1}{T_{4B}}\right)\right],$$
(9)

and solving for T_{4B} gives,

$$T_{4B} = \left[T_{4A}^{-1} - \frac{R}{Q_0} ln \left[\left(\overline{\frac{\overline{t_A}}{t_B}} \right)^q \right] \right]^{-1}.$$ (10)

Now, pause to consider how TBC B, might survive longer than A. It could grow TGO at a slower rate, meaning that B's q will be smaller. Or, TBC B, may be capable of handling the strains produced by a larger TGO. It could also be that TBC B, is inherently tougher, or that it was manufactured with lower residual strains. To encompass all these possibilities, the system is modeled by adjusting the lifetime parameter so that,

$$\overline{t_B} \rightarrow \overline{t_B'} = \overline{t_A} - \overline{\Delta t} = \overline{t_A} - \left(\overline{t_B} - \overline{t_A} \right) = 2 \cdot \overline{t_A} - \overline{t_B}.$$ (11)

Substituting into Equation (10), and recalling that $M_I = \overline{t_1} / \left(2\overline{t_1} - \overline{t_2} \right)$, leaves,

$$T_{4B} = \left[T_{4A}^{-1} - \frac{R}{Q_0} ln \left[\left(M_I \right)^q \right] \right]^{-1}.$$ (12)

And finally, subtracting T_{4A} from both sides produces,

$$\Delta T_4 = \left[T_{4A}^{-1} - \frac{R}{Q_0} ln \left[\left(M_I \right)^q \right] \right]^{-1} - T_{4A}.$$ (13)

Recall that Figure 1(d), showed that M_I is a linear function of E_R. Therefore, Equation (13) calculates the change in T_4 achievable, as a function of the exchange rate and initial T_4 temperature. This relationship is plotted in Figure 3, by assuming a reasonable value of $T_4 = 1,600$ K (Ref. 3).
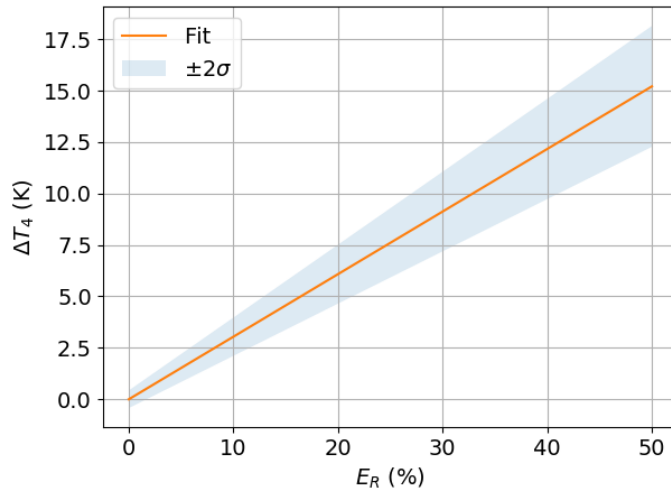

Figure 3.—TBC durability increases with the exchange rate, and can be traded for an increase in turbine entry temperature.

4.0   GTE Fuel Flow Reduction

Holding all other variables constant, increasing T_4 increases the amount of thrust produced, and fuel consumed, by a GTE. If a designer wishes to keep thrust constant, the increased thrust produced by increasing T_4, can be traded for a smaller GTE core. For turbofan configurations, this results in a larger bypass ratio, and it is well known that increasing the bypass ratio reduces thrust specific fuel consumption (TSFC). A lower TSFC implies that the GTE requires less fuel to produce a unit amount of thrust.

Therefore, the increased T_4 capability achieved by producing more durable TBCs, can be used to save operational fuel costs for a GTE. The fuel savings are calculated by referring to turbofan models that include loss parameters. This paper utilizes the model found in "Elements of Gas Turbine Propulsion," (Ref. 3) where a complete list of equations may be found. The parameters dealing directly with T_4, fuel flow and thrust are presented herein. Note that Table II lists all parameters and their values used in this analysis.

The fuel to air ratio of the GTE is,

$$f = \frac{\tau_\lambda - \tau_r \tau_c}{\eta_b \, h_{PR} / c_{pc} \, T_0 - \tau_\lambda}, \tag{14}$$

where,

$$\tau_\lambda = \frac{c_{pt} T_4}{c_{pc} T_0}. \tag{15}$$

TABLE II.—GTE MODEL PARAMETERS

Parameter	Units
M_0	0.9
T_0	216.7 K
γ_c	1.4
c_{pc}	1.004 kJ/kg·K
γ_t	1.3
c_{pt}	1.239 kJ/kg·K
h_{PR}	42,800 kJ/kg
π_{dmax}	0.98
π_b	0.98
π_n	0.98
π_{fn}	0.98
e_c	0.9
e_f	0.88
e_t	0.91
η_b	0.99
η_m	0.98
P_0/P_{19}	0.9
π_c	20
π_f	2.3
$\dot{m}_{fan}$	960 kg/s

Specific thrust is,

$$\frac{F}{\dot{m}_0} = \frac{a_0}{1+\alpha}\left[(1+f)\frac{V_9}{a_0} - M_0 + (1+f)\cdot\frac{R_t T_9 V_9}{R_c T_0 a_0}\frac{1-P_0/P_9}{\gamma_c}\right]$$
$$+ \frac{\alpha\cdot a_0}{1+\alpha}\left[\frac{V_{19}}{a_0} - M_0 + \frac{T_{19}V_{19}}{T_0 a_0}\frac{1-P_0/P_9}{\gamma_c}\right], \tag{16}$$

and the total mass flow is,

$$\dot{m}_0 = \dot{m}_c + \dot{m}_f. \tag{17}$$

Here $\dot{m}_c$ is the mass flow through the GTE core and $\dot{m}_f$ is the mass flow through the fan. Finally, the bypass ratio is,

$$\alpha = \frac{\dot{m}_f}{\dot{m}_c}. \tag{18}$$

Fuel flow as a function of ΔT_4, for a constant thrust is produced by using the parameter values in Table II and the model equations from (Ref. 3).

To calculate the fuel savings, assume that a typical, twin-engine commercial aircraft accrues around 3,000 flight hours per year and that the GTE's turbine blades are replaced once in that time. The results from Figure 4(a) can therefore be converted to fuel savings per aircraft per year, using a fuel cost of $4 per gallon. Finally, the linearized fuel savings per ΔT_4 are expressed as fuel savings versus the exchange rate.

There are now expressions for estimated fuel savings and manufacturing costs, both as functions of the exchange rate. It is now straightforward to calculate the actual expenditure. Fuel savings increase linearly with exchange rate, but manufacturing costs increase at a non-linear rate and therefore the costs eventually overcome the savings achieved. Figure 4 shows the actual expenditure as a function of exchange rate.

The optimum exchange rate is determined by maximizing the lower error bound for the actual savings curve. Doing so shows that an exchange rate of around 28 percent saves approximately $8.45k per twin engine commercial aircraft per year. Extrapolating this to the nearly 5,500 Boeing 737s in service today, would mean a cost savings of $46.5M per year. Recall that these expected savings are based on the lower bound error curve in Figure 4.

The figures quoted here are purely representative. Take for example, Figure 5, which shows the average savings for several different remanufacturing costs per TBC component. As expected, reducing manufacturing costs produced a positive impact on the savings achievable. This model's sensitivity to a large number of parameters means that any specific savings estimate requires high fidelity models for 1) manufacturing costs, 2) TBC failure and 3) GTE performance. Changes to any of these parameters will directly impact the actual savings achievable. Nevertheless, the theoretical analysis provided herein indicates that developing advanced NDT techniques to assess the remaining useful life in TBC components can produce substantial economic benefits to the aeronautical community.
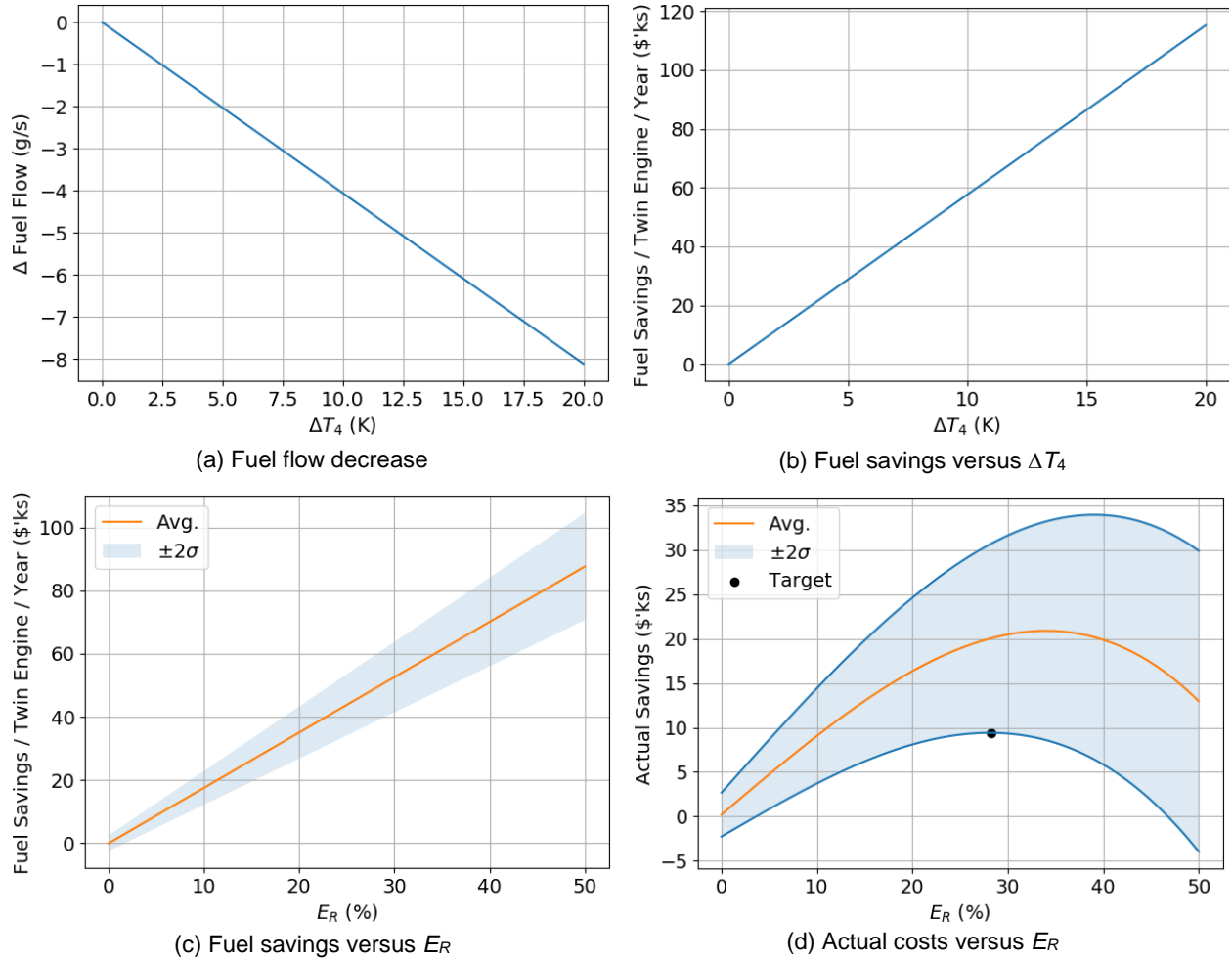
(a) Fuel flow decrease

(b) Fuel savings versus ΔT_4

(c) Fuel savings versus E_R

(d) Actual costs versus E_R

Figure 4.—Increased TBC durability is traded for increased T_4, which is used to increase the GTE bypass ratio, ultimately reducing fuel flow (a). The reduction in required fuel flow can be used to calculate fuel savings for twin engined aircraft over a typical flight year as a function of both ΔT_4 (b) and E_R (c). This cost savings is compared to the manufacturing costs needed to achieve the reduced fuel flow, which produces a curve for the actual savings per year (d).
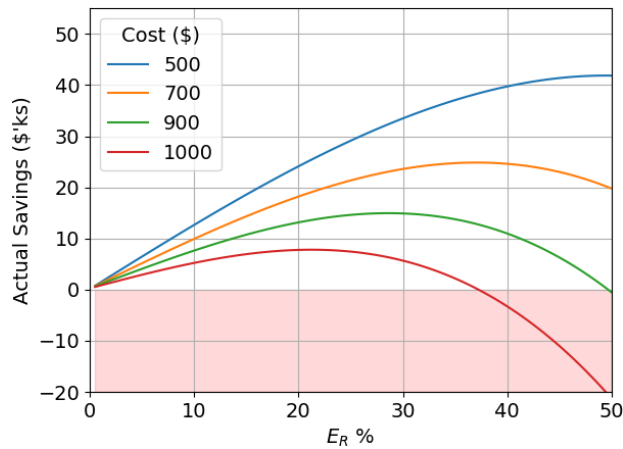

Figure 5.—Achievable cost savings are directly impacted by the cost to remanufacture TBC components. Reducing the manufacturing costs is critical to maximizing savings.

5.0 Conclusion

This paper has outlined a procedure to calculate GTE fuel cost savings, as a function of the manufacturing exchange rate of TBC coated turbine blades. Higher fidelity manufacturing, TBC and GTE models will produce results better tailored to specific aircraft and GTE configurations. However, the conclusion of this paper remains the same: a focused research effort should develop NDT techniques capable of determining the expected remaining useful life in TBC systems.

Suitable NDT techniques will require full field imaging capabilities with a millimeter or less spatial resolution. Furthermore, the ideal technique should be capable of measuring residual strains. TBCs that contain large residual strains post manufacture, will not be able to handle significant TGO growth. Conversely, TBCs with minimal residual strains will last longer. Residual strains in TBCs are largest at the bond coat / top coat interface, and therefore the NDT technique must be able to image through the top coat material.

Unfortunately, powerful optical NDT techniques such as digital image correlation (DIC), are not able to image through the optically opaque TBC ceramic. Commonly used x-ray techniques, such as XRD or XCT, are both time consuming and computationally expensive. Infrared and thermographic imaging is a possibility. It is easy to envision imaging TBCs cool directly after manufacturing, for example. Yet, infrared imaging is typically better suited to finding manufacturing defects that are already present, such as TBC delamination, as opposed to quantitative residual strain analysis.

Therefore, the NDT technique most likely to determine remaining useful life in TBCs is either THz or submillimeter based. It is not a far stretch to imagine adapting current airport security body scanner technology for this purpose. This fast imaging technique could be coupled with Microwave Enhanced Photoelasticity (MEP) (Refs. 13 to 15), in order to image TBC residual strains. MEP replaces optical imaging systems, used in traditional photoelasticity, with microwave sources and detectors. This allows MEP instruments to image residual strain fields in optically opaque, dielectric materials, such as ceramics.

Reviewing the NASA Aeronautics Research Mission Directorate's Strategic Implementation Plan from 2017 (Ref. 16), shows that this work falls within Strategic Thrust 3a: Ultra-Efficient Commercial Vehicles - Subsonic Transport. Developing the NDT technology proposed in this paper specifically supports NASA's near-term objective to reduce aircraft fuel consumption by 50 percent, before 2025. Furthermore, this work integrates with the existing Thrust 3 research theme; Modeling, Simulation and Test Capability, by providing novel experimental tools and methods to quickly improve vehicle capabilities. Ultimately, a renewed focus on NDT technique development will enable NASA to continue providing positive, real-world outcomes for the aerospace industry.

References

1. K. Hünecke, Jet Engines: Fundamentals of Theory Design and Operation (Wiltshire: Airlife, 1997).
2. Rolls Royce Plc., The Jet Engine (West Sussex: John Wiley, 2005).
3. J.D. Mattingly, Elements of Gas Turbine Propulsion (New York: McGraw-Hill, 1996).
4. A. Evans, D. Mumm, J. Hutchinson, G. Meier, and F. Pettit, "Mechanisms controlling the durability of thermal barrier coatings," Prog. Mater. Sci. **46**, 505 – 553 (2001).
5. R. Vaßen, M. O. Jarligo, T. Steinke, D. E. Mack, and D. Stöver, "Overview on advanced thermal barrier coatings," Surf. Coatings Technol. **205**, 938 – 942 (2010).
6. B. Gleeson, "Thermal barrier coatings for aeroengine applications," J. Propuls. Power **22**, 375 – 385 (2006).

7. R. Ragupathy, R. Mishra, and R. Misal, "Life analysis of TBC on an aero engine combustor based on in-service failures data," J. Aerosp. Sci. Technol. **63**, 158–164 (2011).

8. R.G. Wellman and J.R. Nicholls, "A review of the erosion of thermal barrier coatings," J. Phys. D: Appl. Phys. **40**, 293–305 (2007).

9. S. M. Meier, D. M. Nissley, and K. D. Sheffler, "Thermal barrier coating life prediction model development," NASA Tech. Memo. 1991-189111 (1991).

10. E. Busso, L. Wright, H. Evans, L. McCartney, S. Saunders, S. Osgerby, and J. Nunn, "A physics-based life prediction methodology for thermal barrier coating systems," Acta Materialia **55**, 1491 – 1503 (2007).

11. E.P. Busso and Z.Q. Qian, "A mechanistic study of microcracking in transversely isotropic ceramic-metal systems," Acta Materialia **54**, 325 – 338 (2006).

12. E. Busso, J. Lin, S. Sakurai, and M. Nakayama, "A mechanistic study of oxidation-induced degradation in a plasma-sprayed thermal barrier coating system: Part i: model formulation," Acta Materialia **49**, 1515 – 1528 (2001).

13. P. Schemmel, G. Diederich, and A. J. Moore, "Measurement of direct strain optic coefficient of YSZ thermal barrier coatings at GHz frequencies," Opt. Express **25**, 19968–19980 (2017).

14. P. Schemmel and A.J. Moore, "Monitoring stress changes in carbon fiber reinforced polymer composites with GHz radiation," Appl. Opt. **56**, 6405–6409 (2017).

15. P. Schemmel, G. Diederich, and A. J. Moore, "Direct stress optic coefficients for YTZP ceramic and PTFE at GHz frequencies," Opt. Express **24**, 8110–8119 (2016).

16. "NASA Aeronautics Strategic Implementation Plan 2017 Update," https://www.nasa.gov/aeroresearch/strategy.